npj | aging

Article

Published in partnership with the Japanese Society of Anti-Aging Medicine

https://doi.org/10.1038/s41514-025-00228-x

Dysregulations of C1QA, C1QB, C1QC and C5AR1 as candidate biomarkers of vascular dementia

Yawen Xu[1,2,8], Hailing Zhang[1,8], Xuehao Jiao[1,8], Yanbo Zhang[3], Ge Yin[1], Cui Wang[2], Zengkan Du[4], Meng Liang[1], Xin Gao[1], Zhengsheng Gu[1], Yan Jiang[5,6], Bingying Du[1,7] ✉ & Xiaoying Bi[1] ✉

Vascular dementia (VaD) is the second most common cause of dementia. Few bioinformatic analysis has been done to explore its biomarkers. This study aimed to excavate potential biomarkers for VaD using bioinformatic analysis and validate them at both animal and patient levels. Based on microarray data of GSE122063, bioinformatic analysis revealed 502 DEGs in the frontal and 674 DEGs in the temporal cortex of VaD patients. Afterward, the hub genes between two regions, including C1QA, C1QB, C1QC, and C5AR1, were dugout. Interestingly, compared with sham mice or controls, the above four complements were highly expressed in the cortices of VaD animals and in the peripheral serum of VaD patients. Moreover, receiver operating characteristic curve analysis conformed to good diagnostic powers of these complements, with C1QB having the most prominent capacity (AUC = 0.799, 95%CI 0.722–0.875). That means the complements, especially subunits of C1Q, might be used as specific early VaD diagnostic biomarkers.

Vascular dementia (VaD) is the second most common cause of neurocognitive disorders after Alzheimer's disease (AD) and accounts for ~15–30% of dementia cases globally[1]. Neurodegenerative pathologies of VaD and AD often coexist in dementia patients[2]. The clinical manifestations of it are recommended now to extend the spectrum of VaD from subjective cognitive dysfunction and mild cognitive impairment to dementia[3,4]. Besides, the various cerebrovascular changes in VaD made it even more challenging to elucidate the mechanisms of VaD[5]. Although much progress has been made, systematic and effective treatments for VaD are yet to be identified[6,7]. Therefore, due to its mixed pathologies and complex comorbidity with other diseases, to date, no standard treatments for VaD are available worldwide[1].

Owing to the deepening of neuropathology and neuroimaging studies, research on VaD has been more in-depth. It is reported that many VaD patients develop a predominant frontal dysexecutive syndrome in their early stage before profound memory impairment occurs[8]. Neuroimaging studies have demonstrated that medial temporal atrophy is one of the pathological features of VaD[9,10]. Recent observations further suggest that entirely independent of AD pathology, VaD has a vascular basis for neuronal atrophy in both the temporal and frontal cortices[5]. The best strategy recommended for brain sampling of VaD diagnosis would include sections from frontal and temporal levels[11].

Messenger RNA (mRNA) has attracted much interest since the 1960s[12]. Transcripts and proteins are encoded by less than 20,000 genes and could be detected by human transcriptome. The development of RNA sequencing (RNA-seq) helps to better understand the mechanisms that give rise to alternative transcripts and their translation[13]. The technique is especially prominent in quick detection, massive data production, and storage in public databases[14]. Thanks to the advances in sequencing and high-throughput DNA microarray techniques, numerous genes related to AD development have been identified, such as Amyloid β (A4) precursor protein (APP), Presenilin 1(PSEN1), Presenilin 2 (PSEN2), and Apolipoprotein E(APOE)[15]. However, relatively little attention has been paid to VaD in the field of genetic research[16]. Therefore, the objective of the present study is to dig out potential biomarkers of VaD using bioinformatic analysis and then validate at both animal and patient levels.

[1]Department of Neurology, Shanghai Changhai Hospital, Second Military Medical University, Shanghai, PR China. [2]Department of Neurology, Dalian Municipal Central Hospital Affiliated to Dalian University of Technology, Dalian, PR China. [3]Department of Psychiatry, Faculty of Medicine and Dentistry, University of Alberta, Edmonton, AB, Canada. [4]Faculty of Basic Medical Sciences, Second Military Medical University, Shanghai, PR China. [5]School of Pharmacy, Second Military Medical University, Shanghai, PR China. [6]Department of Oral and Maxillofacial-Head Neck Oncology, Shanghai Ninth People's Hospital, College of Stomatology, Shanghai Jiao Tong University School of Medicine, Shanghai, PR China. [7]State Key Laboratory of Medical Neurobiology, Institute for Translational Brain Research, MOE Frontiers Center for Brain Science, MOE Innovative Center for New Drug Development of Immune Inflammatory Disease, Fudan University, Shanghai, PR China. [8]These authors contributed equally: Yawen Xu, Hailing Zhang, Xuehao Jiao. ✉e-mail: 15800614142@163.com; bixiaoying2013@163.com

Results

Filtering DEGs in VaD

In brief, 8 VaD and 11 CT elderly were included in our study (Table S1). Besides, one VaD patient (Sample 381#) had four frontal and temporal samples, and the other 18 participants had two frontal and temporal models. Therefore, 80 specimens were collected. We found 502 and 674 DEGs in the frontal cortex (Fig. S1A, 274 upregulated and 228 downregulated) and temporal cortex (Fig. S2A, 402 upregulated and 272 downregulated) via the Limma package in R studio.

Constructing PPI networks of DEGs

To build PPI networks, 502 and 674 DEGs from frontal and temporal cortices were input into the String database separately (Figs. S1 and S2). With a combined score ≥0.4, there were 220 nodes, 738 edges in the frontal network (Fig. S1B), 163 nodes, and 543 edges in the temporal network (Fig. S2B). Then, MCODE was applied for further clustering of modules. Two top clusters with the highest scores in two networks were extracted (Figs. S1C and S2C. frontal cortex: 27 genes and 114 pairs, temporal cortex: 15 genes and 82 teams). After that, via analysis of the Cytohubba plug-in, we mined the top 20 hub genes from both cortices. The 20 "seed genes" in the frontal cortex are CCR5, CD163, C5AR1, FCGR2A, TLR2, ITGAM, FPR1, GNG13, NMU, SST, DRD4, ADORA3, PNOC, ALB, MPO, TLR5, CCL2, C1QA, C1QB, CD1B (Fig. S1D), in the temporal cortex are PTPRC, CCR5, TLR2, CD163, CCL2, IL18, IL2, TLR5, VEGFA, FCGR2A, IDO1, CCR1, C1QB, C1QA, ITGB2, C5AR1, C1QC, CYBB, SYK and VSIG4 (Fig. S2D) according to score rankings. The heatmaps of differential expression profiles of top 20 genes in frontal and temporal regions of both VaD or CT groups were exhibited in Fig. 1.

Analyzing GO enrichment of DEGs

Both 502 and 674 DEGs of two cortices were analyzed by DAVID database in the three GO aspects: BP, CC, and MF. The top10 elements of each GO term were listed in Fig. S3A. The results showed that for frontal DEGs, 1) BP was particularly enriched in the inflammatory response, positive regulation of angiogenesis, organ regeneration, response to interleukin-6, extracellular matrix organization etc.; 2) CC were enriched in extracellular region, collagen trimer, blood microparticle, plasma membrane, neuronal cell body etc.; 3) MF were significantly enriched in neuropeptide hormone activity, hormone activity, transmembrane receptor protein tyrosine kinase activity, TNF-activated receptor activity, and oxygen binding etc. Besides, another Cytoscape plug-in, ClueGO, was further employed to order the non-redundant biological terms for classification in a functionally grouped network (Fig. S3B). The clustered network was identified as functionally linked based on its *kappa* score level (≥0.3). The results indicated that subset biological terms were mostly enriched in positive regulation of neuron death (37.8%) and regulation of neuron death (13.5%).

For temporal DEGs, 1) BP were particularly enriched in inflammatory response, oxidation-reduction process, natural killer cell activation, VEGF receptor signaling pathway, VEGF signaling pathway etc.; 2) CC were

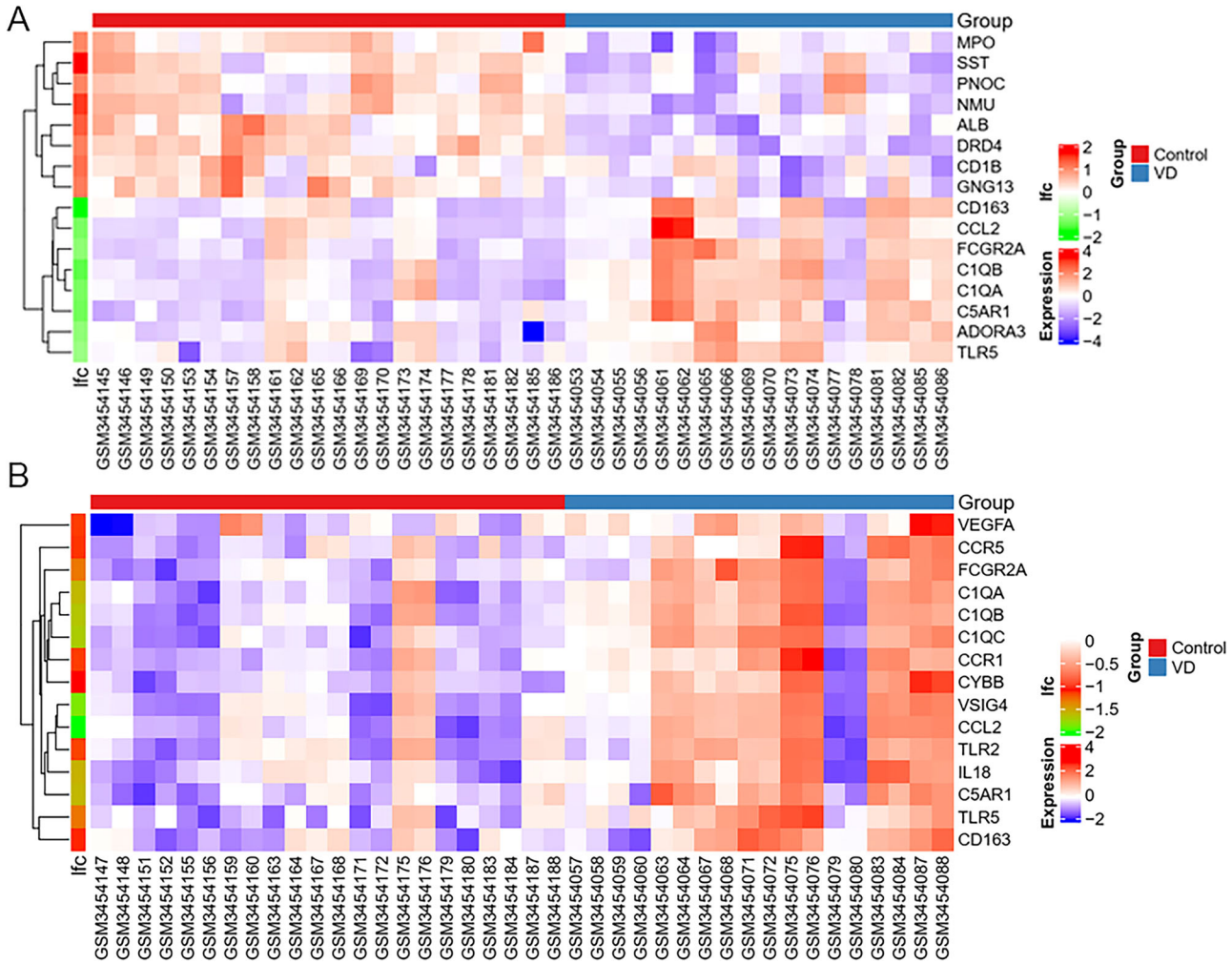

Fig. 1 | Differential expression heatmaps of genes. The heatmaps of the differential expression profile of top 20 genes in the frontal (**A**) and temporal (**B**) regions for both VaD and CT groups. The vertical axis represents the selected 20 genes; the horizontal axis represents the sample numbers. Lfc $\log_2$ fold change.

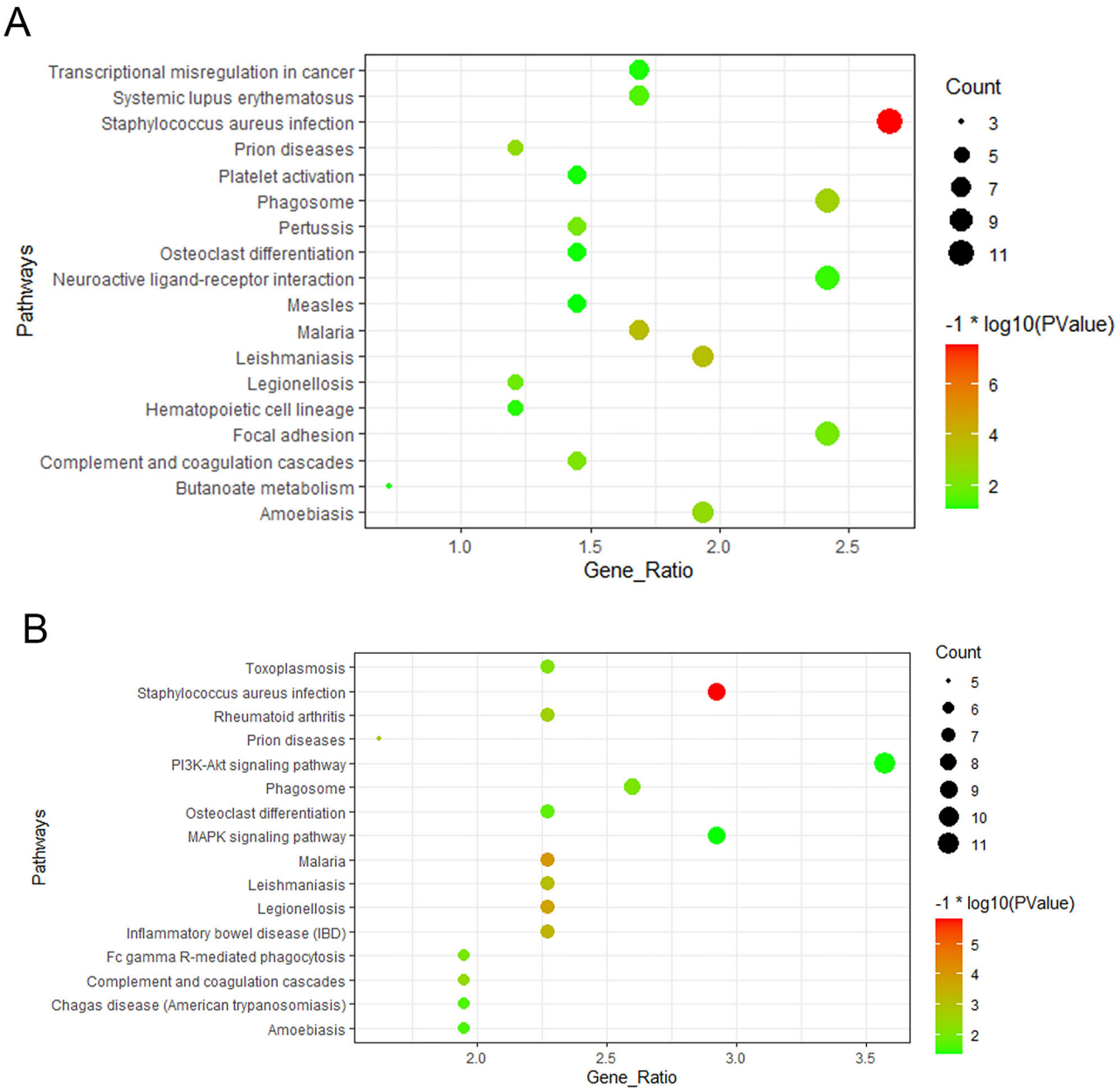

Fig. 2 | KEGG pathway enrichment analysis. KEGG pathway analysis of frontal (**A**) and temporal (**B**) DEGs by DAVID. The vertical axis represents the pathway name; the horizontal axis represents the Gene Ratio, which indicates the ratio of relative gene numbers in a pathway to the numbers of all the annotated genes in the path. A higher Gene Ratio reflects a higher level of enrichment. The size of the points is proportional to the number of critical targets in the ways, and the colors of the dots refer to the *P* values.

enriched in collagen trimer, integral component of plasma membrane, extracellular region, plasma membrane, proteinaceous extracellular matrix etc.; 3) MF were significantly enriched in ATPase activity, coupled, C-C chemokine binding, C3HC4-type RING finger domain binding, ribonuclease activity and chemokine receptor activity etc. (Fig. S4A). The results of ClueGO demonstrated that subset biological terms were mostly enriched in regulation of neutrophil activation death (39.0%) and negative regulation of immune effector process (14.0%, Fig. S4B).

Exploring KEGG pathway enrichment

DAVID database was further used to identify KEGG pathway enrichment of DEGs in the above two regions. There was a total of 18 and 25 KEGG pathways with P value < 0.05 were enriched in frontal and temporal regions, respectively. The results of top10 KEGG pathways in both cortices were picked up and constructed in bubble plot via R Studio (Fig. 2).

Identifying common genes and searching their internal relationships

Frontal and temporal DEGs were imported into Venny 2.1 to seek common genes in two regions (Fig. 3A). 202 common targets were found and the PPI networks (Fig. 3B), core module (Fig. 3C), and hub genes (Fig. 3D) were authenticated as described above. Afterwards, top 20 genes were intersected to KEGG database to sort out matched pathways. As a result, pathways of complement and coagulation cascades, Staphylococcus aureus infection, and neuroactive ligand-receptor interaction were the most related ones. What's more, the chemokine signaling pathway was also included in the matched objects. The KEGG mappers with target genes in colors were shown in Fig. S5.

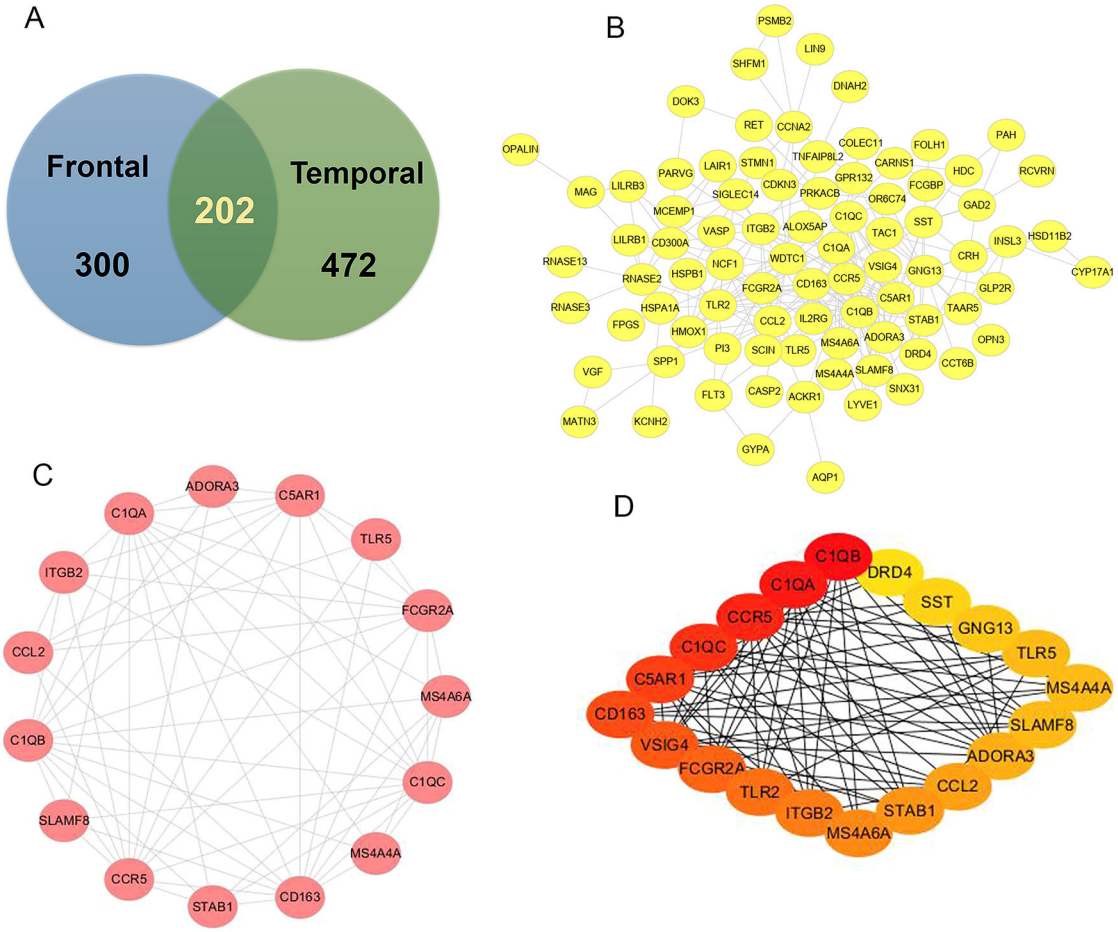

Fig. 3 | PPI network of common DEGs constructed by Cytoscape. A Wayne diagram of 202 DEGs drawn by Venny 2.1. **B** A total of 202 DEGs and their pairs were visualized in the network. **C** The cluster has the highest score in module analysis via MCODE. **D** The PPI network of top 20 hub genes ranked by scores among (**B**). Yellow ellipse nodes: all DEGs; red ellipse nodes: genes in the cluster; red to yellow ellipse nodes: top 20 genes according to their scores; black edges: interactions between genes. DEGs differentially expressed genes, PPI protein-protein interaction.

Expression of cortical C1QA, C1QB, C1QC and C5AR1 mRNA in mice

We first tested the hippocampal-dependent spatial learning and memory by MWM. Figure S6A shows the escape latencies on a training session of 5 days (POD). On the 5th day, compared with the Sham group, a noticeable longer latency was seen with the BCAS group, indicating a significant model-by-treatment interaction (Fig. S6A, $P < 0.001$). Furthermore, on the spatial probe test, mice in the BCAS group had more crossing times in the platform area (Fig. S6C, $P = 0.018$), and more time traveled in the target quadrant (Fig. S6D, $P = 0.011$) than those of Sham groups, while no difference was seen in swim speed ($P = 0.455$) (Fig. S6B). All these measures collectively indicated the cognitive impairment of BCAS mice.

After that, we validated the levels of C1QA, C1QB, C1QC, and C5AR1 in the frontal and temporal cortices by qRT-PCR. Figure 4 shows that all the above four complements-related proteins showed remarkably higher elevated expressions in the BCAS group compared to sham mice. The *P*s between the two groups were 0.035, 0.001,0.004 and 0.045 for C1QA, C1QB, C1QC, and C5AR1 in the frontal cortex, while 0.005, 0.002, 0.008, and 0.011 accordingly in the temporal lobe.

Demographical and clinical characteristics of participants

A total of 64 VaD patients (mean age 66.5 ± 5.1 years; 56.3% women) with sex-/age-matched CTs (mean age 65.2 ± 5.9 years; 53.1% women) were included in this study. As is presented in Table 1, the VaD patients have higher levels of systolic blood pressure (SBP, $P = 0.018$), diastolic blood pressure (DBP, $P = 0.015$), white blood count (WBC, $P = 0.007$), and low-density lipoprotein cholesterol (LDL-C, $P = 0.042$), while a lower level of high-density lipoprotein cholesterol (HDL-C, $P < 0.001$) than those of the CTs. Other parameters including pulse pressure (PP), fasting blood glucose (FBG), hemoglobin A1c (HbA1c), red blood cell (RBC), hemoglobin (Hb), neutrophil to lymphocyte ratio (NLR), total cholesterol (TC), triglyceride (TG), total bilirubin (TB) showed no significant differences (all *P*s > 0.05).

The MoCA scores of VaD patients and healthy controls were 18.6 ± 3.3 and 28.5 ± 1.3, separately ($P < 0.001$). Then, we tested the C1QA, C1QB, C1QC, and C5AR1 in the serum with ELISA. Interestingly, as revealed by Fig. 5A–D, consistent with the animal results, VaD patients had higher levels of C1QA ($P < 0.001$), C1QB ($P = 0.008$), C1QC ($P < 0.001$), and C5AR1 ($P < 0.001$). Moreover, the diagnostic ability of these four genes was subsequently evaluated by ROC curves. Figure 5E exhibited that the AUCs were 0.658 (95%CI, 0.560–0.756), 0.799 (95%CI, 0.722–0.875), 0.780 (95%CI, 0.693–0.867) and 0.681 (95%CI, 0.588–0.775) for C1QA, C1QB, C1QC and C5AR1, separately, with C1QB has the most prominent diagnostic capacity.

Discussion

VaD, characterized by white matter lesions (WMLs), is a progressive neurodegenerative disorder that can only be controlled by prevention and treatment in the early stage[5]. Although progress has been made in understanding the pathology, some uncertainties remain[6]. Accepted diagnostic criteria and disease-modifying managements are still paucities[17]. Therefore, with the widespread application of microarray technology and bioinformatics analytical software, the current research was mainly focused on exploiting new biomarkers of VaD.

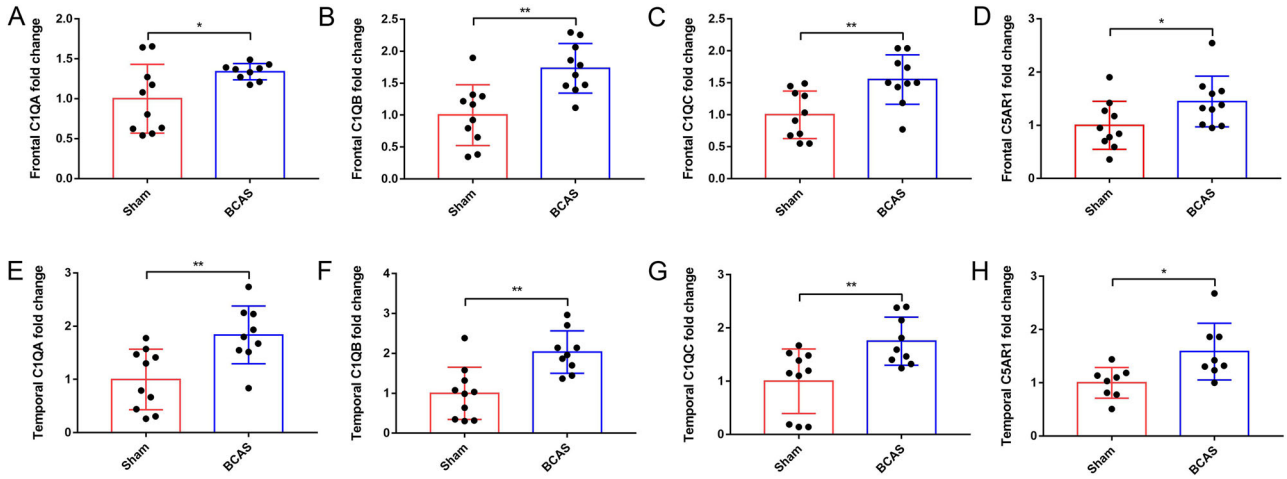

Fig. 4 | Cerebral mRNA expression of C1QA, C1QB, C1QC, and C5AR1. Cerebral mRNA expressions of C1QA, C1QB, C1QC, and C5AR1 in the frontal (**A**–**D**) and temporal (**E**–**H**) cortices for both BCAS and Sham mice. Data are presented as means ± SD. $n = 10$ per group. $^{*}P < 0.05$, $^{**}P < 0.01$ compared to the Sham group. BCAS bilateral common carotid artery stenosis.

Table 1 | Characteristics of study subjects

Characteristics	VCI group	control	*P* value
Age (years)	66.5 ± 5.1	65.2 ± 5.9	0.153
Percent women (%)	56.3	53.1	0.312
SBP (mmHg)	158.2 ± 32.4	150.7 ± 28.5	0.018
DBP (mmHg)	94.6 ± 20.3	86.3 ± 17.9	0.015
PP (mmHg)	57.3 ± 10.6	60.5 ± 14.2	0.205
WBC(×109/L)	6.2 ± 1.2	5.5 ± 1.3	0.007
RBC (×1012/L)	4.8 ± 0.5	4.8 ± 0.5	0.916
Hb (g/L)	148.5 ± 15.3	147.9 ± 15.2	0.855
NLR	1.9 ± 0.8	1.7 ± 0.7	0.351
FBG (mmol/L)	5.8 ± 0.7	5.7 ± 0.7	0.505
HbA1c (%)	5.8 ± 0.4	5.9 ± 0.5	0.716
TB(μmol/L)	13.3 ± 3.8	14.0 ± 4.6	0.521
TC (mmol/L)	5.5 ± 1.1	5.4 ± 0.9	0.424
TG (mmol/L)	1.8 ± 1.3	1.5 ± 0.9	0.287
LDL-C (mmol/L)	3.6 ± 1.0	3.3 ± 0.7	0.042
HDL-C (mmol/L)	1.4 ± 0.3	1.7 ± 0.5	<0.001
MoCA score	18.6 ± 3.3	28.5 ± 1.3	<0.001
C1QA (μg/mL)	224.1 ± 85.9	268.6 ± 93.0	0.008
C1QB (μg/mL)	162.9 ± 46.8	112.0 ± 41.8	<0.001
C1QC (ng/mL)	539.6 ± 138.5	457.1 ± 34.9	<0.001
C5AR1 (ng/mL)	190.6 ± 53.2	151.4 ± 61.7	<0.001

VaD vascular dementia, *SBP* systolic blood pressure, *DBP* diastolic blood pressure, *PP* pulse pressure, *WBC* white blood cell, *RBC* red blood cell, *Hb* hemoglobin, *NLR* neutrophil to lymphocyte ratio, *FBG* fast blood glucose, *HbA1c* hemoglobin A1c, *TB* total bilirubin, *TC* total cholesterol, *TG* triglyceride, *LDL-C* low-density lipoprotein cholesterol, *HDL-C* low-density lipoprotein cholesterol, *MoCA* Montreal Cognitive Assessment.

The Venn diagram indicated that genes from complement systems such as C1QA, C1QB, C1QC, and C5AR1 occupied a big part of common top 20 hub genes. The complement system is composed of more than 30 proteins[18]. The recognition component of the C1 complex, C1q, is composed of three distinct polypeptide chains, A, B, and C[19]. It is reported that C1q played pivotal roles in the clearance of apoptotic cells and cellular debris, inhibition of phagocyte-derived proinflammatory cytokines expression[20–22], and protection of stress-induced neuronal damage[23,24]. It is thereby estimated that consistent with maintaining homeostasis, neuronal injuries and neuroinflammation could increase the synthesis of C1q[25]. Indeed, a mouse model of AD has demonstrated that with age and amyloid accumulation, the level of C1q in CNS usually increases[24]. In contrast, C1q deficiency has been proven to be neuroprotective against AD and hypoxic-ischemic brain injury[26,27]. Besides, evidence has reported the indispensable role of C1q in hypoperfusion-induced WMLs[28,29], which confirmed our results from another aspect. Another research also found that C1QA, C1QB, C1QC, and C5AR1 were the hub genes of the carotid atherosclerosis (CAS) and VaD, which may reveal a new relationship between CAS and VaD[30]. Consistent with our findings, a recent bioinformatic study by Xu et al. identified that C1QA, C1QB C1QC were the top three essential genes keeping healthy brain aging[31].

Furthermore, researchers found that during the early stages of neurodegeneration, the presence of C1q was beneficial and protective. While with age and injuries progress, complement cascade results in detrimental activities[32–34]. In addition, it is well demonstrated that when the complement cascade activates, C5a generation increases dramatically[35]. Binding to its cellular receptor C5aR, it recruits glial cells, promotes proinflammatory glial polarization and aggravates neuroinflammation[35,36]. Thus, the function of complement in the aging and neurodegenerative brain remains to be excavated. They have great potential to be candidate biomarkers for early diagnosis and measurement of neurodegenerative dysfunctions, including VaD.

According to our screening results of GO enrichment, the inflammatory response was the key biological process in VaD development. Microglia are considered key elements in initiating an inflammatory reaction after injury. When activated, they are capable of secreting various cytokines, such as interleukin (IL)-1β, IL-6, and tumor necrosis factor (TNF)-α[37], and the latter exacerbate white matter injury and even deteriorate the cognitive function of VaD[37,38]. Our previous research has also demonstrated robust microglia activation, followed by significantly increased secretion of IL-1β, IL-6, and TNF-α in VaD mice. When administrated with an inhibitor of microglial activation minocycline, microglial activation and proinflammatory cytokines were alleviated, and cognition of VaD mice was reversed[39]. Besides, by using $C1qa^{FL/FL}$: $Cx3cr1Cre^{ERT2/WganJ}$ mice, Fonseca et al. found that CX3CR1-expressing microglia are the dominant source of C1q in the neurodegenerative murine brain[18]. Complement receptors are also expressed by inappropriately activated microglia, and they play a detrimental role in normal aging and neurodegenerative pathology[40–42]. These collectively indicated that aberrant microglial activation is an early signal of pathological abnormality in VaD. Inhibiting microglial-mediated inflammation and complement accumulation is crucial in VaD management[18,21,39,43,44].

Just as discussed above, microglia were the crucial resource of complement and its receptor[21]. Injurious role of inappropriate activated

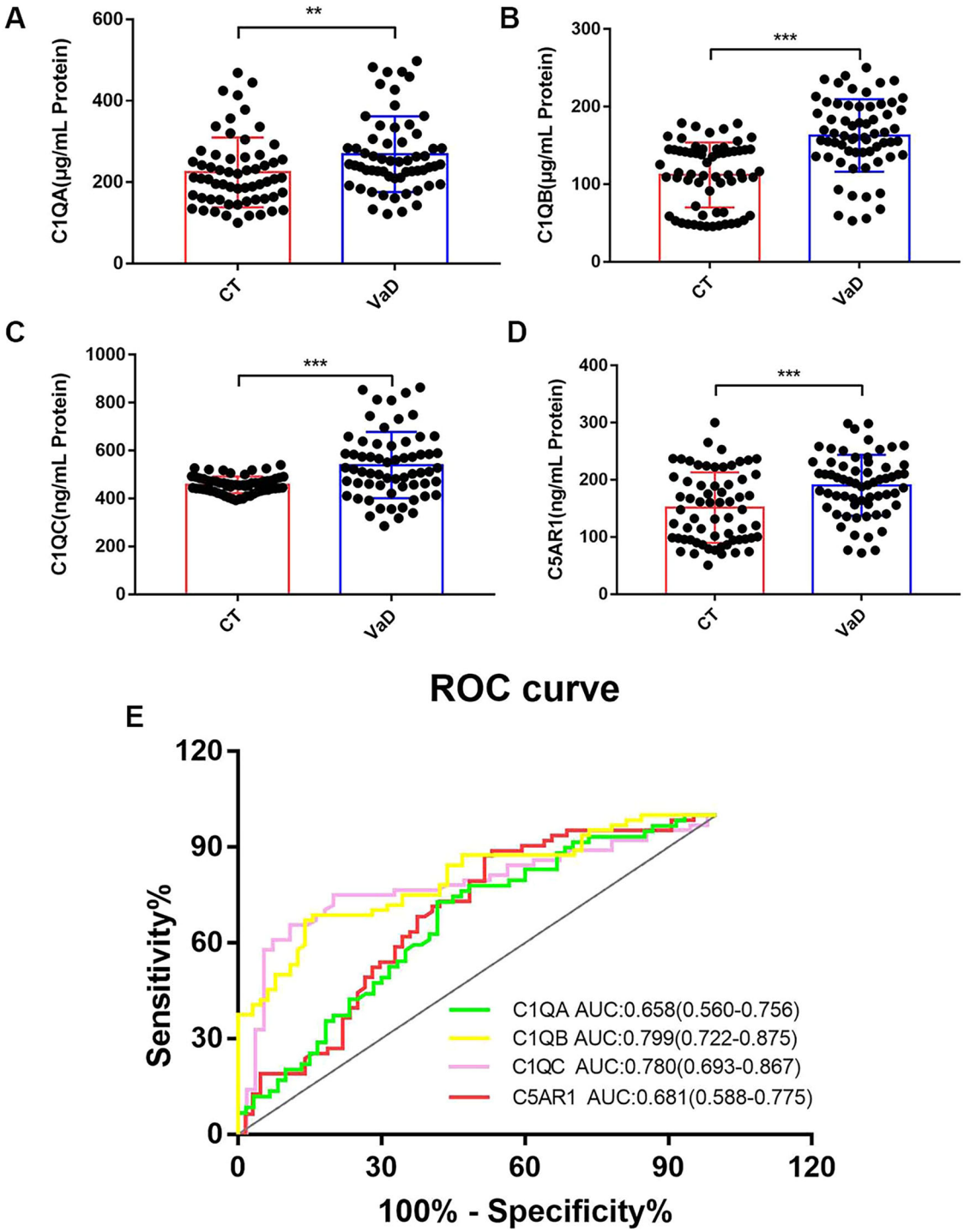

Fig. 5 | Serum expression and diagnostic values of C1QA, C1QB, C1QC, and C5AR1. Serum expressions (**A**–**D**) and diagnostic values (**E**) of C1QA, C1QB, C1QC, and C5AR1 for VaD. Data are presented as means ± SD. $n = 64$ per group. $^{**}P < 0.01$, $^{***}P < 0.001$ compared to the CT group. CT controls, VaD vascular dementia, ROC receiving operating characteristic, AUC area under the curve.

microglia and complement play in neurodegenerative pathology, for example, AD, and related pathways were already demonstrated by genome-wide association studies[40,42,45]. McKay et al., who generated the gene expression dataset have further supported the similarity of gene expression profiles between AD and VaD, whose data indicated considerable overlap between DEGs in AD and VaD patients[46]. However, no exact evidence has been targeted validated between complement and VaD yet. What's more, except for frontal lobe, we also identified the differential expression profiles in temporal lobe, and further identified the role of activated microglia and complement in two regions. Targeting the characteristics of different brain regions, the biological pathways or hub genes found in the current study helps to better elucidate VaD mechanisms.

Besides, chemokine signaling pathway was another enriched pathway in KEGG analysis. Critical for microglia-neuron crosstalk, Fractalkine, also known as CX3CL1, is constitutively expressed by neurons. While its receptor, CX3CR1, is highly expressed in microglia in CNS[47]. Our and others' previous studies have implicated the neurotoxic role of CX3CL1/CX3CR1 axis played in ischemic stroke[48–50]. We found that

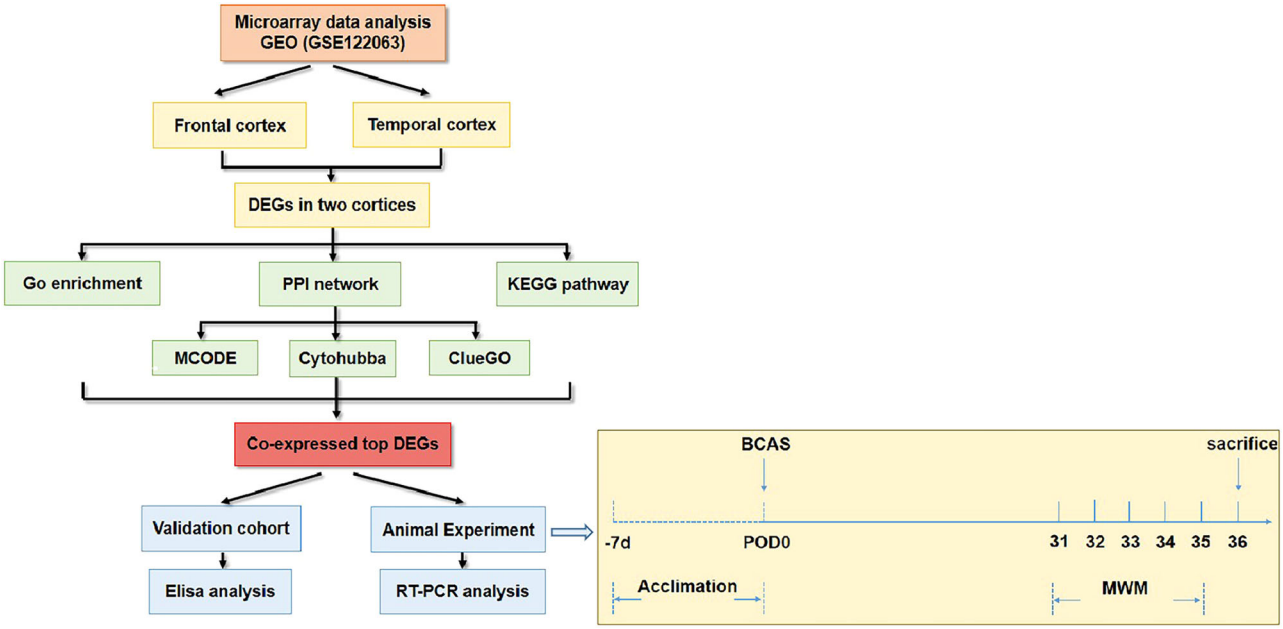

Fig. 6 | The flow chart of this study. GEO Gene Expression Omnibus, DEGs differentially expressed genes, GO Gene Ontology, PPI protein-protein interaction, KEGG Kyoto Encyclopedia of Genes and Genomes, BCAS bilateral common carotid artery stenosis, POD post-operation day, MWM Morris water maze.

intracerebroventricular injection with CX3CR1 antibody reduced the microglia activation and myelination loss in cortex and hippocampus, and cognitive impairment of VaD mice was ameliorated[43]. We speculated that chemokine signaling pathways have the potential to function as novel therapeutic targets in VaD as well.

To our knowledge, this is by far the first study not only evaluated the central and peripheral complement levels of VaD, but also confirmed good diagnostic powers of C1QB and C1QC for VaD. Considering the lack of biomarkers for VaD, we foresee that besides current laboratory testing, abnormal manifestations of complement, inflammatory, or even chemokine cytokines might have the potential to provide new insights for VaD. However, it is a pity that VaD patients combined with AD were not singled out and performed subgroup analysis. Further studies are needed to prove whether combined several indices might improve the accuracy and effectiveness of the VaD prognosis, and how the diagnostic value is the above complement-related proteins in AD.

Materials and methods

A schematic diagram of the workflow is shown in Fig. 6.

Microarray data acquisition

Gene expression profile data of GSE122063 were obtained from Gene Expression Omnibus (GEO) (https://www.ncbi.nlm.nih.gov/geo), an open-access database with a significant amount of gene expression data[51]. The platform of GSE122063 was GPL16699, Agilent-039494 SurePrint G3 Human GE v2 8x60K Microarray 039381. The microarray data included frontal and temporal cortices from 8 VaD patients and 11 non-demented controls (CT). The tissues were collected from the University of Michigan Brain Bank. CT cases had no infarcts in the autopsied hemisphere, and VaD cases had low Braak staging.

Data preprocessing and differential gene analysis

The conversion of raw data into normalized format was realized by GEO2R (https://www.ncbi.nlm.nih.gov/geo/geo2r/), an online analytical tool available in GEO[52]. Limma package from Bioconductor software (http://www.bioconductor.org/) was utilized for the identification of the differentially expressed genes (DEGs) between the VaDs and CTs[53]. Thresholds of adjusted P and $|\log_2 FC|$ values were set to 0.05 and 1 separately for significant DEGs. Afterward, we employed a volcano plot to visualize the results of DEGs.

PPI networks constructing and topological features analysis of DEGs

The Search Tool for the Retrieval of Interacting Genes (String) is a database that provides information predicting and analyzing experimental interactions of proteins with a solid computational ability[54]. The significantly DEGs of frontal and temporal lobes were inputted into String and visualized in PPI networks. The assessment of protein-protein association intensity with a medium confidence score (≥0.4) was chosen for further exploration. After exporting the result in a tab-separated value (TSV) format, Cytoscape software (version 3.6.2) was used to construct the PPI networks.

Molecular Complex Detection (MCODE) is one of the Cytoscape clustering algorithms to check notable modules of PPI networks[55]. We set the advanced options in MCODE: degree cutoff = 2, max. Depth = 100, K-core = 2, and node score cutoff = 0.2. Besides, the top 20 genes from frontal and temporal lobes were chosen according to scores calculated by Cytohubba, a plug-in of Cytoscape[56]. After the detection of hub genes, expression profiles of DEGs in both groups were shown by heatmaps. In addition, we adopted ClueGO, another Cytoscape plug-in, to decipher functionally grouped gene ontology and pathway annotation networks[57].

Gene ontology and pathway enrichment analysis of DEGs

We hired the Database for Annotation, Visualization, and Integrated Discovery (DAVID, https://david.ncifcrf.gov/, ver. 6.8) for Gene ontology (GO) and Kyoto Encyclopedia of Genes and Genomes (KEGG) pathway analysis of DEGs. GO enrichment was primarily for the unification of biology[58]. It is now a valuable tool to systematically classify the unique biological properties of a specific list of genes[59]. Three biological functions, including physical process (BP), cellular component (CC), and molecular part (MF) of GO analysis, were performed via DAVID. DAVID was conducted for KEGG analysis, which dealt with genomes, diseases, biological pathways, drugs, and chemical materials[60]. The cutoff criteria were set as P values of 0.05, and bubble plots were employed to show the results for further analysis.

Common genes identifying and potential pathways reanalyzing

Common genes of two cortices were sought via software Venny 2.1 (available online: https://bioinfogp.cnb.csic.es/tools/venny/), and a Wayne

diagram was drawn to authenticate the results. The common targets were then picked up to construct PPI networks, build core modules, and extract hub genes described above. Afterward, top 20 genes were intersected to the KEGG database to sort out the best-matched pathways and visualized by KEGG mappers in colors.

Animal experiments

All procedures were approved by the Animal Care Committee of the Second Military Medical University and by the Animal Research Guidelines for the care and use of laboratory animals. The study was carried out in compliance with the ARRIVE guidelines.

Surgery procedures

Ten C57BL/6 male mice (aged 10–12 weeks, weighing 25 to 30 g) were acclimated for a week under a 12-h light/12-h dark cycle with free access to food and water ad libitum. Then, mice were randomly assigned to a sham group and bilateral common carotid artery stenosis (BCAS) group. To induce BCAS, mice were anesthetized with isoflurane, and the steel spring microcoil (0.18-mm internal diameter, 2.5 mm total length, Sawane Spring Co., Ltd, Shizuoka, Japan) was twined by rotating around both right and left common carotid artery (CCA)[61]. Sham animals were given a skin incision, and their CCAs were exposed. After surgery, animals were returned to the standard cage to recover, and this date was defined as post-operation day (POD) 0.

Morris water maze

Morris water maze (MWM) was performed 30 days after surgery to evaluate the spatial learning and memory of animals as described previously[39,43]. In short, the circle tank was divided into four quadrants, and a 6-cm-diameter hidden platform was submerged 2 cm below the water surface in the target quadrant (northwest) of the tank. During the first 5 days of the hidden platform test (POD31-POD35), each mouse was gently released from one of the four quadrants and given 60 s to find the platform. The activity of the animal in MWM was video-tracked by a video camera (Xinruan Technology Co., Ltd, Shanghai, China), and the escape latencies were recorded. If mice failed to find the platform within 60 s, they were gently guided to the forum and allowed to rest on it for 10 s. Mice were trained four times daily, with inter-trial intervals of more than 15 min. For the long-term spatial probe test on POD36, the platform was removed from the pool, and each animal was released from four different quadrants for 60 s. The swimming speed, times of mice crossing the platform area, and the time spent in the target quadrant were tracked and recorded.

Quantitative real-time RT-PCR (qRT-PCR)

Total RNAs were isolated from both frontal and temporal cortices using TRIzol (Life Technologies Corp., Grand Island, NY, USA) according to the manufacturer's protocols. All RNA isolated was converted into cDNA with SuperScript III transcriptase (Life Technologies Corp.). Quantitative RT-PCR was performed using iTaq Universal SYBR Green Supermix (Bio-Rad) on a CFX 96 Touch Real-Time PCR Detection System. The following human primer sequences were used: XXXX. β-actin (fwd-5′-CTCTCCC TCACGCCATC-3′ and rev-5′-ACGCACGATTTCCCTCTC-3′); C1QA (fwd-5′-CCAGGAGAGTCCATACCAGAA-3′ and rev-5′-GTCCCACTT GGAGATCACTTG-3′); C1QB (fwd-5′-GGCAACCTGTGTGTGAATC TC-3′ and rev-5′-CTCTAGCTTCAAGACTACCCCA-3′); C1QC (fwd-5′-AGAAGCACCAGTCGGTATTCA-3′ and rev-5′-TGCGATGTGTAGTA GACGAAGTA-3′); C5AR1 (fwd-5′-TACCATTAGTGCCGACCGTTT-3′ and rev-5′-CCGGTACACGAAGGATGGAAT-3′). All the expression data were normalized to β-actin.

Human study

This study was approved by the recommendations of the Ethics Committee of Changhai Hospital, the Second Medical University, with written informed consent from all participants, and all experiments were performed in accordance with relevant guidelines and regulations.

Participants' recruitment and data collection

From October 1st to November 30th, 2017, 64 VaD (or significant vascular cognitive impairment) patients and 64 age-/sex-matched control individuals were enrolled. The inclusion criteria of VaD patients were consistent with Guidelines for Diagnosis and Treatment of Chinese Vascular Cognitive Impairment[62]. Trained staff recorded information on demographic characteristics, personal medical history, and educational conditions with standard questionnaires. One of the best widely used instruments, the Montreal Cognitive Assessment (MoCA) scale, was used to evaluate the participants' cognitive functions as previously described[63]. The venous blood samples were collected, and after an overnight fast of more than ten h, serum samples were separated and immediately frozen at −80 °C until the further experiment. The Institutional Review Board approved the protocol of Changhai Hospital, the Second Military Medical University (No. CHEC2018-153).

Enzyme-linked immunosorbent assay

Serum levels of C1QA, C1QB, C1QC, and C5AR1 were measured using an enzyme-linked immunosorbent assay (ELISA) kit (Wodeng Technology Co., Ltd., Shanghai, China) according to the manufacturer's protocol. The optical density (OD) at 450 nm was measured using a microplate reader (Bio-Rad, Richmond, CA). A curve fit was applied to the standard curve according to the manufacturer's manual using Microplate Manager 6 Software (Bio-Rad, Richmond, CA). The unknown concentration of the above complement in each sample was extrapolated from these standard curves.

Statistical analysis

All data were analyzed by SPSS 24.0 and processed with GraphPad Prism 7 (GraphPad Software, Inc., La Jolla, CA). Descriptions of categorical variables were n (%), while continuous variables were expressed as mean ± SD or lower (Q1) and upper (Q3) quartile. For statistical test analysis, a t-test was used to compare continuous parameters between the two groups, and a chi-square was used for categorical variables. Comparison of learning curves between groups was performed with a repeated measures t-test. In addition, the receiving operating characteristic (ROC) curve was plotted, and area under the curve (AUC) was calculated. All tests were two-sided, and significant differences were considered at $P < 0.05$.

Data availability

The datasets generated and/or analyzed during the current study are available in the GEO database (https://www.ncbi.nlm.nih.gov/geo, GSE122063). All other data are available from the corresponding authors upon reasonable request.

Received: 5 August 2024; Accepted: 22 April 2025;
Published online: 25 May 2025

References

1. O'Brien, J. T. et al. Vascular cognitive impairment. *Lancet Neurol.* **2**, 89–98 (2003).
2. Smith, E. E. Clinical presentations and epidemiology of vascular dementia. *Clin. Sci.* **131**, 1059–1068 (2017).
3. Petersen, R. C. & O'Brien, J. Mild cognitive impairment should be considered for DSM-V. *J. Geriatr. Psychiatry Neurol.* **19**, 147–154 (2006).
4. Sachdev, P. et al. Diagnostic criteria for vascular cognitive disorders: a VASCOG statement. *Alzheimer Dis. Assoc. Disord.* **28**, 206–218 (2014).
5. Kalaria, R. N. Neuropathological diagnosis of vascular cognitive impairment and vascular dementia with implications for Alzheimer's disease. *Acta Neuropathol.* **131**, 659–685 (2016).
6. O'Brien, J. T. & Thomas, A. Vascular dementia. *Lancet* **386**, 1698–1706 (2015).

7. Perry, E., Ziabreva, I., Perry, R., Aarsland, D. & Ballard, C. Absence of cholinergic deficits in "pure" vascular dementia. *Neurology* **64**, 132–133 (2005).
8. Desmond, D. W. The neuropsychology of vascular cognitive impairment: Is there a specific cognitive deficit? *J. Neurol. Sci.* **226**, 3–7 (2004).
9. Bastos-Leite, A. J. et al. The contribution of medial temporal lobe atrophy and vascular pathology to cognitive impairment in vascular dementia. *Stroke* **38**, 3182–3185 (2007).
10. Firbank, M. J. et al. Cerebral blood flow by arterial spin labeling in poststroke dementia. *Neurology* **76**, 1478–1484 (2011).
11. Deramecourt, V. et al. Staging and natural history of cerebrovascular pathology in dementia. *Neurology* **78**, 1043–1050 (2012).
12. Brenner, S., Jacob, F. & Meselson, M. An unstable intermediate carrying information from genes to ribosomes for protein synthesis. *Nature* **190**, 576–581 (1961).
13. de Klerk, E., & 't Hoen, P. A. Alternative mRNA transcription, processing, and translation: insights from RNA sequencing. *Trends Genet.* **31**, 128–139 (2015).
14. Vogelstein, B. et al. Cancer genome landscapes. *Science* **339**, 1546–1558 (2013).
15. Guerreiro, R., Brás, J. & Hardy, J. SnapShot: genetics of Alzheimer's disease. *Cell* **155**, 968–968.e1 (2013).
16. Lagunin, A. A. et al. Combined network pharmacology and virtual reverse pharmacology approaches for identification of potential targets to treat vascular dementia. *Sci. Rep.* **10**, 257 (2020).
17. van der Flier, W. M. et al. Vascular cognitive impairment. *Nat. Rev. Dis. Prim.* **4**, 18003 (2018).
18. Fonseca, M. I. et al. Cell-specific deletion of C1qa identifies microglia as the dominant source of C1q in mouse brain. *J. Neuroinflamm.* **14**, 48 (2017).
19. Reid, K. B. & Porter, R. R. Subunit composition and structure of subcomponent C1q of the first component of human complement. *Biochem. J.* **155**, 19–23 (1976).
20. Fraser, D. A., Pisalyaput, K. & Tenner, A. J. C1q enhances microglial clearance of apoptotic neurons and neuronal blebs, and modulates subsequent inflammatory cytokine production. *J. Neurochem.* **112**, 733–743 (2010).
21. Benoit, M. E., Clarke, E. V., Morgado, P., Fraser, D. A. & Tenner, A. J. Complement protein C1q directs macrophage polarization and limits inflammasome activity during the uptake of apoptotic cells. *J. Immunol.* **188**, 5682–5693 (2012).
22. Roumenina, L. T. et al. Functional complement C1q abnormality leads to impaired immune complexes and apoptotic cell clearance. *J. Immunol.* **187**, 4369–4373 (2011).
23. Benoit, M. E. & Tenner, A. J. Complement protein C1q-mediated neuroprotection is correlated with regulation of neuronal gene and microRNA expression. *J. Neurosci.* **31**, 3459–3469 (2011).
24. Benoit, M. E. et al. C1q-induced LRP1B and GPR6 proteins expressed early in Alzheimer disease mouse models, are essential for the C1q-mediated protection against amyloid-beta neurotoxicity. *J. Biol. Chem.* **288**, 654–665 (2013).
25. Holden, S. S. et al. Complement factor C1q mediates sleep spindle loss and epileptic spikes after mild brain injury. *Science* **373**, eabj2685 (2021).
26. Ten, V. S. et al. C1q-deficiency is neuroprotective against hypoxic-ischemic brain injury in neonatal mice. *Stroke* **36**, 2244–2250 (2005).
27. Audrain, M. et al. Integrative approach to sporadic Alzheimer's disease: deficiency of TYROBP in a tauopathy mouse model reduces C1q and normalizes clinical phenotype while increasing spread and state of phosphorylation of tau. *Mol. Psychiatry* **24**, 1383–1397 (2019).
28. Fowler, J. H. et al. Dimethyl fumarate improves white matter function following severe hypoperfusion: involvement of microglia/macrophages and inflammatory mediators. *J. Cereb. Blood Flow Metab.* **38**, 1354–1370 (2018).
29. Sigfridsson, E., Marangoni, M., Hardingham, G. E., Horsburgh, K. & Fowler, J. H. Deficiency of Nrf2 exacerbates white matter damage and microglia/macrophage levels in a mouse model of vascular cognitive impairment. *J. Neuroinflamm.* **17**, 367 (2020).
30. Dongshi, L. et al. Bioinformatic identification of potential biomarkers and therapeutic targets in carotid atherosclerosis and vascular dementia. *Front. Neurol.* **13**, 1091453 (2023).
31. Xu, J., Zhou, H. & Xiang, G. Identification of key biomarkers and pathways for maintaining cognitively normal brain aging based on integrated bioinformatics analysis. *Front. Aging Neurosci.* **14**, 833402 (2022).
32. Rozovsky, I. et al. Selective expression of clusterin (SGP-2) and complement C1qB and C4 during responses to neurotoxins in vivo and in vitro. *Neuroscience* **62**, 741–758 (1994).
33. Fan, R. & Tenner, A. J. Complement C1q expression induced by Abeta in rat hippocampal organotypic slice cultures. *Exp. Neurol.* **185**, 241–253 (2004).
34. Cribbs, D. H. et al. Extensive innate immune gene activation accompanies brain aging, increasing vulnerability to cognitive decline and neurodegeneration: a microarray study. *J. Neuroinflamm.* **9**, 179 (2012).
35. Veerhuis, R., Nielsen, H. M. & Tenner, A. J. Complement in the brain. *Mol. Immunol.* **48**, 1592–1603 (2011).
36. Klos, A. et al. The role of the anaphylatoxins in health and disease. *Mol. Immunol.* **46**, 2753–2766 (2009).
37. Karve, I. P., Taylor, J. M. & Crack, P. J. The contribution of astrocytes and microglia to traumatic brain injury. *Br. J. Pharmacol.* **173**, 692–702 (2016).
38. Fernando, M. S. et al. White matter lesions in an unselected cohort of the elderly: molecular pathology suggests origin from chronic hypoperfusion injury. *Stroke* **37**, 1391–1398 (2006).
39. Du, B. et al. Minocycline ameliorates depressive-like behavior and demyelination induced by transient global cerebral ischemia by inhibiting microglial activation. *Front. Pharmacol.* **10**, 1247 (2019).
40. Hong, S. et al. Complement and microglia mediate early synapse loss in Alzheimer mouse models. *Science* **352**, 712–716 (2016).
41. Hammond, T. R., Marsh, S. E. & Stevens, B. Immune signaling in neurodegeneration. *Immunity* **50**, 955–974 (2019).
42. Wu, T. et al. Complement C3 is activated in human AD brain and is required for neurodegeneration in mouse models of amyloidosis and tauopathy. *Cell Rep.* **28**, 2111–2123.e6 (2019).
43. Du, B. et al. Anti-mouse CX3CR1 antibody alleviates cognitive impairment, neuronal loss and myelin deficits in an animal model of brain ischemia. *Neuroscience* **438**, 169–181 (2020).
44. Guo, T., Fang, J., Tong, Z. Y., He, S. & Luo, Y. Transcranial direct current stimulation ameliorates cognitive impairment via modulating oxidative stress, inflammation, and autophagy in a rat model of vascular dementia. *Front. Neurosci.* **14**, 28 (2020).
45. Hong, S., Dissing-Olesen, L. & Stevens, B. New insights on the role of microglia in synaptic pruning in health and disease. *Curr. Opin. Neurobiol.* **36**, 128–134 (2016).
46. McKay, E. C. et al. Peri-infarct upregulation of the oxytocin receptor in vascular dementia. *J. Neuropathol. Exp. Neurol.* **78**, 436–452 (2019).
47. Ransohoff, R. M. Microgliosis: the questions shape the answers. *Nat. Neurosci.* **10**, 1507–1509 (2007).
48. Fumagalli, S., Perego, C., Ortolano, F. & De Simoni, M. G. CX3CR1 deficiency induces an early protective inflammatory environment in ischemic mice. *Glia* **61**, 827–842 (2013).
49. Tang, Z. et al. CX3CR1 deficiency suppresses activation and neurotoxicity of microglia/macrophage in experimental ischemic stroke. *J. Neuroinflamm.* **11**, 26 (2014).

50. Liu, Y. Z. et al. Role of fractalkine/CX3CR1 signaling pathway in the recovery of neurological function after early ischemic stroke in a rat model. *Life Sci.* **184**, 87–94 (2017).
51. Edgar, R., Domrachev, M. & Lash, A. E. Gene expression omnibus: NCBI gene expression and hybridization array data repository. *Nucleic Acids Res.* **30**, 207–210 (2002).
52. Davis, S. & Meltzer, P. S. GEOquery: a bridge between the Gene Expression Omnibus (GEO) and BioConductor. *Bioinformatics* **23**, 1846–1847 (2007).
53. Ritchie, M. E. et al. Limma powers differential expression analyses for RNA-sequencing and microarray studies. *Nucleic Acids Res.* **43**, e47 (2015).
54. Szklarczyk, D. et al. STRING v11: protein-protein association networks with increased coverage, supporting functional discovery in genome-wide experimental datasets. *Nucleic Acids Res.* **47**, D607–D613 (2019).
55. Bader, G. D. & Hogue, C. W. An automated method for finding molecular complexes in large protein interaction networks. *BMC Bioinform.* **4**, 2 (2003).
56. Lou, W., Ding, B., Xu, L. & Fan, W. Construction of potential glioblastoma multiforme-related miRNA-mRNA regulatory network. *Front. Mol. Neurosci.* **12**, 66 (2019).
57. Bindea, G. et al. ClueGO: a Cytoscape plug-in to decipher functionally grouped gene ontology and pathway annotation networks. *Bioinformatics* **25**, 1091–1093 (2009).
58. Ashburner, M. et al. Gene ontology: tool for the unification of biology. The Gene Ontology Consortium. *Nat. Genet.* **25**, 25–29 (2000).
59. Tiirikka, T., Siermala, M. & Vihinen, M. Clustering of gene ontology terms in genomes. *Gene* **550**, 155–164 (2014).
60. Kanehisa, M., & Goto, S. KEGG: kyoto encyclopedia of genes and genomes. *Nucleic Acids Res.* **28**, 27–30 (2000). Jan 1.
61. Temma, T. et al. Sequential PET estimation of cerebral oxygen metabolism with spontaneous respiration of 15O-gas in mice with bilateral common carotid artery stenosis. *J. Cereb. Blood Flow Metab.* **37**, 3334–3343 (2017).
62. Professional Committee of Cognitive Impairment Diseases of Chinese Medical Doctor Association Neurosurgery Branch, China Vascular Cognitive Impairment Guidelines Writing Group. 2019 guidelines for the diagnosis and treatment of chinese vascular cognitive impairment. *Chin. Med. J.* **99**, 2737–2744 (2019).
63. Du, B. et al. Strong association of serum GSK-3β/BDNF ratio with mild cognitive impairment in elderly type 2 diabetic patients. *Curr. Alzheimer Res.* **16**, 1151–1160 (2019).

Acknowledgements

The authors are grateful to PhD Chen Zhang, Department of Orthopedics, General Hospital of Central Theater Command of Chinese People's Liberation Army, Wuhan, China, for his kind assistance. We also acknowledge the GEO database for their platforms and contributors for uploading their high-quality data. This work was supported by the National Natural Science Foundation of China (NSFC, NO. 81871040 and NO. 82101563), the Natural Science Foundation of Shanghai (22ZR1477100), the Shanghai Health System Talent Training Program (2018BR29), and the Shanghai Talent Development Fund (2021064).

Author contributions

All authors have participated and made substantial contributions to this paper. Y.X. and B.D. contributed to study design. Y.X., G.Y., and C.W. collected the original data and performed the analysis. B.D., Y.X., and X.J. contributed to writing and revisions of the manuscript. Y.Z. and H.Z. contributed to the analysis and interpretation of data. M.L., X.G., and Z.G. performed part of the data collection and analysis. B.D., H.Z., and X.B. contributed to the study supervision, conception, and design. All authors had approved the final manuscript.

Competing interests

The authors declare no competing interests.

Additional information

Supplementary information The online version contains supplementary material available at https://doi.org/10.1038/s41514-025-00228-x.

Correspondence and requests for materials should be addressed to Bingying Du or Xiaoying Bi.